

## Si segregation in polycrystalline Co<sub>2</sub>MnSi films with grain-size control

A. Hirohata, S. Ladak, N. P. Aley, and G. B. Hix

Citation: *Applied Physics Letters* **95**, 252506 (2009); doi: 10.1063/1.3276073

View online: <http://dx.doi.org/10.1063/1.3276073>

View Table of Contents: <http://scitation.aip.org/content/aip/journal/apl/95/25?ver=pdfcov>

Published by the [AIP Publishing](#)

---



## Re-register for Table of Content Alerts

Create a profile.



Sign up today!



## Si segregation in polycrystalline $\text{Co}_2\text{MnSi}$ films with grain-size control

A. Hirohata,<sup>1,a)</sup> S. Ladak,<sup>2,b)</sup> N. P. Aley,<sup>2</sup> and G. B. Hix<sup>3</sup>

<sup>1</sup>Department of Electronics, The University of York, Heslington, York YO10 5DD, United Kingdom

<sup>2</sup>Department of Physics, The University of York, Heslington, York YO10 5DD, United Kingdom

<sup>3</sup>Nottingham Trent University, Burton Street, Nottingham NG1 4BU, United Kingdom

(Received 25 September 2009; accepted 28 November 2009; published online 23 December 2009)

In order to characterize the interface/surface properties of polycrystalline  $\text{Co}_2\text{MnSi}$  Heusler alloy films, grain-size evolution with increasing annealing time has been investigated. Here, samples with nanometer-scale grains have been prepared by our specially-designed sputtering system in order to maximize the interface/surface area. Our well-controlled grains clearly show Si phase segregation. This Si phase becomes conductive near room temperature and may be responsible for the significant decrease in tunneling magnetoresistance previously reported by [Wang *et al.*, Appl. Phys. Lett. **93**, 122506 (2008)]. © 2009 American Institute of Physics. [doi:10.1063/1.3276073]

In order to realize 100% spin polarization induced by spontaneous magnetization at room temperature (RT), half-metallic ferromagnets (HMF) have been widely investigated.<sup>1</sup> The HMF possesses a bandgap  $\delta$  at the Fermi level  $E_F$  only for its minority spins, achieving 100% spin polarization at  $E_F$ . However, to date there has been no experimental report on the half-metallicity at RT which is crucial for future spin-source applications. Among theoretically proposed HMFs, Heusler alloys hold the greatest potential due to their following properties; high Curie temperature (usually above RT), lattice constant matching with major substrates (such as III-V semiconductors and MgO) and large  $\delta$  at  $E_F$  in general. Recently, a magnetic tunnel junction (MTJ) with an epitaxial  $L2_1$ -phase  $\text{Co}_2\text{MnSi}$  film has been reported to show very large tunneling magnetoresistance (TMR) ratios of 70% at RT and 159% at 2 K (Ref. 2). These are the largest TMR ratio obtained in a MTJ with a Heusler alloy film and  $\text{AlO}_x$  barrier. In addition, a MTJ using epitaxial  $\text{Co}_2\text{Fe}(\text{Al},\text{Si})$  films with an epitaxial MgO barrier has been found to double the TMR ratio, with values as high as 150% at RT and 312% at 7 K being reported.<sup>3</sup> Even so, such rapid decrease in the TMR ratio with increasing temperature does not follow the simple temperature dependence of the saturation magnetization [empirically known to follow the Bloch formula  $T^{3/2}$  (Ref. 4)]. This suggests that a small fraction of atomically disordered phases cannot be ignored in the spin-polarized electron transport at a finite temperature. The elimination of such disordered phases, especially near the barrier interface, should improve the TMR ratios further and should realize half-metallicity at RT. In this study we fabricated polycrystalline  $\text{Co}_2\text{MnSi}$  films with controlled grain sizes by sputtering in order to investigate the dependence of both the magnetic and structural properties on the annealing time. In particular, the surface/interface phase segregation has been studied.

Polycrystalline films were prepared using a HiTUS sputtering system to deposit with full control of the grain size.<sup>5</sup>  $\text{MgO}(001)$  substrates were cleaned with acetone and annealed at 573 K for 20 min at a base pressure of

$3 \times 10^{-5}$  Pa. The plasma was generated by an rf field at  $3 \times 10^{-1}$  Pa Ar pressure and steered onto the target with a dc bias ( $V_T$ ) ranging from  $-250$  to  $-990$  V, which controlled the deposition rate. This resulted in the change of the average grain size of as-deposited films. The smaller grains are expected to exhibit significant properties due to grain-boundary effects, while the larger ones exhibit properties closer to those of the bulk material. The  $\text{Co}_2\text{MnSi}$  films were grown at 573 K, and the film thickness maintained at 23 nm with a 2 nm thick Ru capping layer. The chemical compositions of the samples were estimated from energy dispersive x-ray spectroscopy (EDX). These films were systematically annealed at 760 K for 3 to 9 h. This is the maximum temperature we could achieve for annealing and is near the annealing temperature used in the earlier studies.<sup>2</sup> After each annealing, magnetization curves were measured by using a PMC alternating gradient force magnetometer (AGFM) at RT. Grain size analysis was also carried out by transmission electron microscopy (TEM), and the crystal structures were characterized by grazing incidence X-ray diffraction (XRD).

The chemical composition of the  $\text{Co}_2\text{MnSi}$  Heusler alloy films were measured by EDX and the data is listed in Table I. The Co concentrations are found to decrease with increasing target bias voltage  $V_T$ , while the Mn concentrations increase to give an almost stoichiometric composition for  $V_T = -750$  and  $-990$  V. It should be noted that the Si concentration stays almost the same with the variation of  $V_T$  and are intentionally maintained to be slightly lower than the stoichiometric value by 5~8%. After 9 h annealing, a few large segregated particles were observed of sub-micron size by scanning electron microscopy (SEM). By focusing the EDX analysis onto these particles, Si-rich phases were found even

TABLE I. Chemical compositions of the films measured by EDX. Those for segregated particles are shown in parenthesis.

Bias voltage [V]	Co [at. %]	Mn [at. %]	Si [at. %]
-250	67.48(21.03)	12.78(18.87)	19.74(60.10)
-500	60.19(51.36)	21.87(27.77)	17.94(20.87)
-750	51.39(28.27)	31.27(22.02)	17.35(49.71)
-990	49.39(34.96)	33.83(28.07)	16.79(36.97)

a)Electronic mail: ah566@ohm.york.ac.uk.

b)Present Address: Department of Physics, Blackett Laboratory, Imperial College, Prince Consort Road, London SW7 2AZ, England.

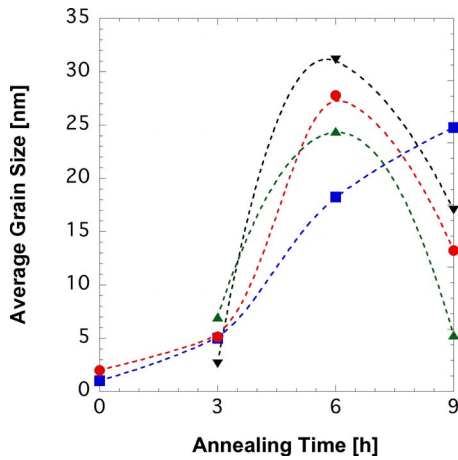


FIG. 1. (Color online) Evolution of average grain sizes of  $\text{Co}_2\text{MnSi}$  films grown at  $V_T = -250$  (black triangles),  $-500$  (green triangles),  $-750$  (blue squares), and  $-990$  V (red circles) with respect to the annealing period. Dotted lines are guides to the eye.

in these Si-poor matrices. The values are shown in parenthesis in Table I.

Observable nanoparticles are initially formed only for two as-deposited films grown at higher values of  $V_T$  as shown in Fig. 1. The average grain sizes of these films were measured to be 1.01 and 1.99 nm for  $V_T = -750$  and  $-990$  V, respectively (see Fig. 2). For each analysis over 300 grains were measured in order to obtain a reliable average grain-size.<sup>5</sup> After 3 h annealing at 760 K, crystalline formation takes place for all the samples forming grains with sizes ranging from 2.59 nm ( $V_T = -250$  V) to 6.97 nm ( $V_T = -500$  V). After 6 h annealing the average grain size increases further and reach a maximum, ranging between 18.26 and 31.11 nm for  $V_T = -750$  V and  $-250$  V, respectively. This increase agrees with the well-established grain evolution for the HiTUS system that the grain size becomes larger with increasing bias.<sup>5</sup> However, additional annealing for 9 h in total, decreases the grain sizes, which suggests some changes in the  $\text{Co}_2\text{MnSi}$  grains, such as minor phase segregation. For the smaller initial grains, the decrease of the grain sizes is more prominent.

XRD results shown in Fig. 3 further support both the formation of  $\text{Co}_2\text{MnSi}$  and minor phase segregation. A  $\text{Co}_2\text{MnSi}(220)$  peak is observed at  $2\theta = 45.70^\circ$  for the film grown at  $V_T = -990$  V and annealed for 9 h, clearly showing the  $\text{Co}_2\text{MnSi}$  matrix formation. The lattice constant of the  $\text{Co}_2\text{MnSi}$  film is estimated to be 0.5619 nm, which is within a 1% mismatch of the reported bulk value 0.56540 nm.<sup>6</sup> A

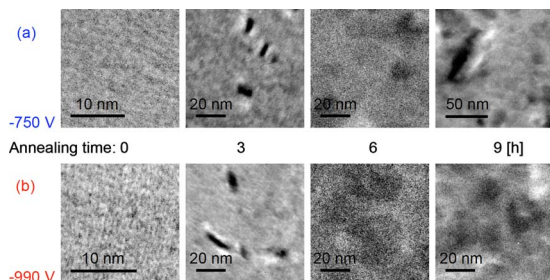


FIG. 2. (Color online) TEM images of polycrystalline  $\text{Co}_2\text{MnSi}$  films grown at (a)  $V_T = -750$  and (b)  $-990$  V. The grain-size evolution is shown with increasing annealing period from 0 to 9 h.

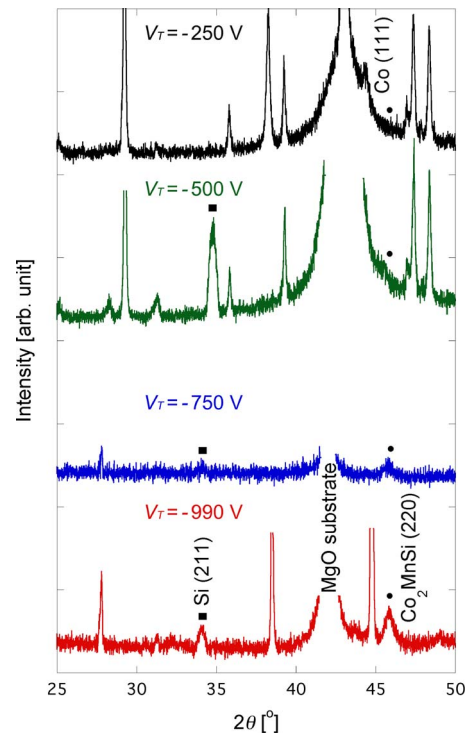


FIG. 3. (Color online) XRD patterns for the 5 h annealed  $\text{Co}_2\text{MnSi}$  films grown at  $V_T = -250$  (black line),  $-500$  (green line),  $-750$  (blue line), and  $-990$  V (red line).  $\text{Co}_2\text{MnSi}$  peaks are indicated with circles and Si peaks are shown with squares.

small  $\text{Co}_2\text{MnSi}(220)$  peak is also visible for  $V_T = -750$  V, however, the peak almost disappears with decreasing magnitude of  $V_T$ . Our XRD sensitivity, however, does not allow us to characterize the remaining films as well as to evaluate the ordering of the  $\text{Co}_2\text{MnSi}$  matrix. This is partially because the grain size is very small as discussed above, which broadens the diffraction peaks in accordance with the Scherrer equation. In our samples, amorphous phases may be present even after annealing as the initial average grain size is below 2 nm. Also some of the smaller particles can be indicative of the presence of an amorphous phase. Such amorphous phases cannot be clearly confirmed by XRD. A Si(211) peak appears for  $V_T = -500$  V at  $2\theta = 33.27^\circ$ , supporting the Si phase segregation observed by the EDX analysis. Although the EDX results in Table I do not show significant Si segregation for the film grown at  $V_T = -500$  V, the XRD clearly shows Si segregation. Minor Si segregation is also observed for the larger value of  $V_T$ , indicating that all the films studied suffer from Si phase segregation. For the lowest  $V_T$ , a Co(111) peak becomes prominent at  $2\theta = 44.38^\circ$  due to the excessive Co concentration as supported by the EDX data in Table I.

Figure 4(a) shows the magnetization curves of the  $\text{Co}_2\text{MnSi}$  films at RT as a function of the annealing period. All the films exhibit almost no magnetic moment at RT before annealing, which agrees with the small initial grain sizes ( $< 2$  nm). The values of the saturation magnetization saturate after around 2 h annealing for the films grown at  $V_T = -250$  and  $-750$  V, which agrees with the above optimized annealing condition. For the two remaining films the saturation magnetization increases monotonically. The value of the saturation magnetization is almost saturated after 5 h annealing. For these samples, the measured magnetic moment per formula unit is less than 65% of the calculated

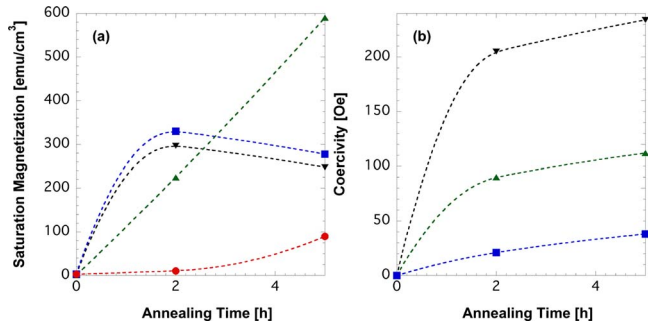


FIG. 4. (Color online) Annealing-time dependence of (a) saturation magnetization and (b) coercivity for the  $\text{Co}_2\text{MnSi}$  film grown at  $V_T = -250$  (black triangles),  $-500$  (green triangles),  $-750$  (blue squares), and  $-990$  (red circles) V. Dotted lines are guides to the eye.

value from a generalized Slater–Pauling curve ( $5 \mu_B/\text{f.u.}$ ).<sup>6</sup> For the  $\text{Co}_2\text{MnSi}$  film with an average grain size of 18 nm, corresponding to the sample grown at  $V = -750$  V, the volume of the bulk  $\text{Co}_2\text{MnSi}$  matrices is calculated to be 54% of the total volume. This corresponds to a three-monolayer-thick disordered surface or interface region as previously reported for epitaxial films.<sup>7</sup> This is also consistent with data from X-ray magnetic circular dichroism studies in similar Co-based Heusler alloy films.<sup>6,8</sup> In addition, for our sputtering system, the packing density of similar films has been measured to be approximately 90%.<sup>9</sup> Therefore about 49% of the saturation magnetization is expected as compared with that of an epitaxial  $\text{Co}_2\text{MnSi}$  film. Because our Heusler alloy films are not fully  $L2_1$  ordered, an additional decrease in the saturation magnetization is also expected. This means that the samples with small grain sizes are dominated by surface/interface properties as compared with epitaxial films. It should be noted that the purpose of this study is not to maximize the saturation magnetization with the perfect  $L2_1$  structure but to maximize the area of the interface/surface of  $\text{Co}_2\text{MnSi}$  polycrystalline grains. Additionally, the coercivity  $H_C$ , determined from the magnetization curves measured at RT [Fig. 4(b)], decreases with increasing target bias and hence increasing grain size. The film grown at  $V_T = -990$  V shows a coercivity of 16 Oe, which is comparable with that for a highly ordered  $\text{Co}_2\text{MnSi}$  film.<sup>10</sup> This provides further evidence that the bulk regions of the  $\text{Co}_2\text{MnSi}$  grains are highly ordered.

These results suggest that two types of behavior exist in the films. The films with smaller grains have their magnetic behavior dominated by the grain boundaries, while those with larger grains exhibit bulk properties. In particular the structural characterization by XRD shows significant Si phase segregation, which may be responsible for the decrease in the grain sizes after about 5 h annealing as observed from the TEM analysis. Since Si phase segregation was observed at the surface of all the  $\text{Co}_2\text{MnSi}$  films with

Si-poor concentrations, this may also occur in epitaxial Heusler films with much larger grains. Here Si segregated nanoparticles at the Heusler/tunnel barrier interfaces become almost insulating at low temperature where very large TMR ratios are observed. Si normally behaves as a conductor at RT, and therefore opens additional transport paths for a spin-independent tunneling current across Heusler alloy/barrier interfaces. This results in a significant decrease in TMR ratios as observed for most epitaxial tunnel junctions with  $\text{Co}_2\text{MnSi}$  (Ref. 2) and  $\text{Co}_2\text{Fe}(\text{Si}, \text{Al})$  (Ref. 3) Heusler alloy films. Si segregation can be avoided by intentionally reducing the Si concentrations in a few monolayers near the interfaces and surfaces in such Heusler alloy films. As theoretically predicted, the  $B2$  disordered structure does not disrupt the half-metallicity in some cases.<sup>11</sup> Such an interfacial treatment may maintain the half-metallicity at RT resulting in significant TMR ratios at RT.

In summary, chemical composition analysis has shown that Si phase segregation occurs at the surface of  $\text{Co}_2\text{MnSi}$  sputtered films with nanometer-scale grains after annealing and occurs for all grain sizes. Based on our detailed analysis of the grain-sizes, the annealing condition is optimum at 760 K for 6 h. Even under this condition, segregated nanoparticles with Si concentrations up to 60% are observed by EDX. Such minor phase segregation is difficult to detect by macroscopic measurements such as magnetic studies and XRD as bulk effects dominate these measurements especially for the case of epitaxial films. Our findings provide a way to improve interface properties of Heusler alloy films to achieve the half-metallicity at RT.

The authors would like to thank Professor K. O’Grady of the University of York for the use of his facilities, fruitful discussions and proof-reading the manuscript.

<sup>1</sup>*Half-Metallic Alloys*, edited by I. Galanakis and P. H. Dederichs (Springer, Berlin, 2005).

<sup>2</sup>Y. Sakuraba, J. Nakata, M. Oogane, H. Kubota, Y. Ando, A. Sakuma, and T. Miyazaki, *Jpn. J. Appl. Phys., Part 2* **44**, L1100 (2005).

<sup>3</sup>W. Wang, H. Sukeyawa, R. Shan, and K. Inomata, *Appl. Phys. Lett.* **93**, 122506 (2008).

<sup>4</sup>H. Schneider, G. Jacob, M. Kallmayer, H.-J. Elmers, M. Cinchetti, B. Balke, S. Wurmehl, C. Felser, M. Aeschlimann, and H. Adrian, *Phys. Rev. B* **74**, 174426 (2006).

<sup>5</sup>M. Vopsaroiu, M. J. Thwaites, S. Rand, P. J. Grundy, and K. O’Grady, *IEEE Trans. Magn.* **40**, 2443 (2004).

<sup>6</sup>A. Hirohata, M. Kikuchi, N. Tezuka, K. Inomata, J. S. Claydon, Y. B. Xu, and G. van der Laan, *Curr. Opin. Solid State Mater. Sci.* **10**, 93 (2006).

<sup>7</sup>A. Hirohata, H. Kurebayashi, S. Okamura, M. Kikuchi, T. Masaki, T. Nozaki, N. Tezuka, and K. Inomata, *J. Appl. Phys.* **97**, 103714 (2005).

<sup>8</sup>A. Hirohata, H. Kurebayashi, S. Okamura, T. Masaki, T. Nozaki, M. Kikuchi, N. Tezuka, K. Inomata, J. S. Claydon, and Y. B. Xu, *J. Appl. Phys.* **97**, 10C308 (2005).

<sup>9</sup>N. P. Aley and K. O’Grady (unpublished).

<sup>10</sup>L. J. Singh, Z. H. Barber, Y. Miyoshi, W. R. Branford, and L. F. Cohen, *J. Appl. Phys.* **95**, 7231 (2004).

<sup>11</sup>G. H. Fecher and C. Felser, *J. Phys. D* **40**, 1582 (2007).